Protein Science (1997), 6:637–648. Cambridge University Press. Printed in the USA.

Structure characterization of the central repetitive domain of high molecular weight gluten proteins. I. Model studies using cyclic and linear peptides

ALARD A. VAN DIJK,[1,4] LOURENS L. VAN WIJK,[1] ALEXANDRA VAN VLIET,[2] PARVEZ HARIS,[3,5] ERIC VAN SWIETEN,[1] GODEFRIDUS I. TESSER,[2] AND GEORGE T. ROBILLARD[1]

[1]Department of Biochemistry and Biophysical Chemistry and the Groningen Biomolecular Sciences and Biotechnology Institute, University of Groningen, Nijenborgh 4, 9747 AG Groningen, The Netherlands
[2]Department of Organic Chemistry, Catholic University of Nijmegen, Toernooiveld 1, 6525 ED Nijmegen, The Netherlands
[3]Department of Protein and Molecular Biology, Royal Free Hospital School of Medicine, University of London, Rowland Hill Street, London, NW3 2PF, United Kingdom

(RECEIVED July 31, 1996; ACCEPTED December 10, 1996)

Abstract

The high molecular weight (HMW) proteins from wheat contain a repetitive domain that forms 60–80% of their sequence. The consensus peptides PGQGQQ and GYYPTSPQQ form more than 90% of the domain; both are predicted to adopt β-turn structure. This paper describes the structural characterization of these consensus peptides and forms the basis for the structural characterization of the repetitive HMW domain, described in the companion paper. The cyclic peptides cyclo-[PGQGQQPGQGQQ] (peptide 1), cyclo-[GYYPTSPQQGA] (peptide 2), and cyclo-[PGQGQQGYYPTSPQQ] (peptide 3) were prepared using a novel synthesis route. In addition, the linear peptides $(PGQGQQ)_n$ (n = 1, 3, 5) were prepared. CD, FTIR, and NMR data demonstrated a type II β-turn structure at QPGQ in the cyclic peptide 1 that was also observed in the linear peptides $(PGQGQQ)_n$. A type I β-turn was observed at YPTS and SPQQ in peptides 2 and 3, with additional β-turns of either type I or II at GAGY (peptide 2) and QQGY (peptide 3). The proline in YPTS showed considerable *cis/trans* isomerization, with up to 50% of the population in the *cis*-conformation; the other prolines were more than 90% in the *trans* conformation. The conversion from *trans* to *cis* destroys the type I β-turn at YPTS, but leads to an increase in turn character at SPQQ and GAGY (peptide 2) or QQGY (peptide 3).

Keywords: cyclic and linear peptides; gluten proteins; repetitive proteins; structural characterization

High molecular weight proteins from wheat are a homologous group of storage proteins. Their amino acid sequence can be divided into three domains, a large central domain (500–700 residues) flanked by two smaller domains at the N- and C-terminus (Shewry et al., 1994). The central domain forms 60–80% of the sequence and is completely built from the consensus peptides PGQGQQ, GYYPTSPQQ, and GQQ; the first two form more than 90% of the repetitive domain (Anderson & Greene, 1987; Shewry et al., 1994) and both are predicted to adopt a β-turn conformation (Tatham et al., 1990). In y-type HMW proteins, the second proline in the GYYPTSPQQ repeat motif is often replaced by a leucine. The repetitive domain is thought to consist of a large series of β-turns that organize in a β-spiral structure (Shewry et al., 1994); this idea is supported by scanning tunneling microscopic images of HMW Dx5 (Miles et al., 1991). In order to understand the relevant structural aspects of the HMW repetitive domain, it is necessary to develop detailed structural knowledge. The most straightforward way to do this is via model peptides that mimic the HMW repeat motifs. This approach has been used by Tatham et al. (1990) using short linear peptides representing the HMW consensus sequences. CD and FTIR data showed little secondary structure in aqueous solutions, which results from a lack of conformational restriction; in fact, this is the reason why cyclic peptides are used commonly to characterize turn structures (Perczel & Hollósi, 1996). In this

Reprint requests to: G.T. Robillard, Department of Biochemistry and Biophysical Chemistry and the Groningen Biomolecular Sciences and Biotechnology Institute, University of Groningen, Nijenborgh 4, 9747 AG Groningen, The Netherlands; e-mail: G.T.Robillard@chem.rug.nl.

[4]Present address: Gist Brocades N.V. Postbus 1, 2600 MA, Delft, The Netherlands.

[5]Present address: Department of Biological Sciences, De Montfort University, Hawthorn Building, The Gateway, Leicester, LE1 9BH, England.

Abbreviations: AcOH, acetic acid; BuOH, *n*-butanol; DCC, dicylohexyl-carbodiimide; DCM, dichloro-methane; DIPCDI, diisopropyl-carbodiimide; DIPEA, diisopropyl-ethylamine; DMF, N,N′-dimethyl-formamide; Fmoc, 9-fluorenyl-methoxycarbonyl; Fmoc-OSu, Fmoc-N-hydroxysuccinimide ester; FTIR, fourier transform infrared; HMW, high molecular weight; HOBt, 1-hydroxybenzotriazole; HSQC, heteronuclear single quantum coherence; Nin, ninhydrin; NMM, N-methylmorpholine; OAll, allylester; pTOS, *para*-toluene-sulfonic acid; ROESY, rotating frame overhauser effect spectroscopy; TBTU, O-benzotriazole-N,N,N′N′-tetramethyluronium tetrafluoroborate; TDM, N,N,N′,N′-tetramethyl-4,4′-diaminodiphenylmethane; TFA, trifluoro-acetic acid; TOCSY, total coherence spectroscopy; Trt, trityl.

paper, we describe a novel synthesis route for cyclic peptides and the structural analysis of both cyclic and linear peptides representing the HMW consensus sequences.

Results

Peptide synthesis

Cyclic peptides (Fig. 1) were synthesized starting from a γ-linked glutamyl residue as described in Materials and methods; Figure 2 shows the synthesis scheme for cyclo-[PGQGQQPGQGQQ]. After coupling of the first residue to the resin, a glycine was added at the carboxy-terminus to circumvent the problem of racemization during the final cyclization step. After synthesis of the rest of the peptide, it was cyclized on the resin, reducing the formation of linear oligopeptides that would normally occur in solution. Cleavage from the resin converted the linker glutamic acid to glutamine (Fig. 2); the acid labile protecting groups were removed simultaneously. Peptide 2 was designed initially as cyclo-YYPTSPQQG, but this peptide could not be cyclized because of steric hindrance by the bulky protecting groups on the two tyrosines; the N-terminal addition of an alanine and a glycine solved this problem. The linear peptides $(PGQGQQ)_{1,3,5}$ were prepared using standard Fmoc chemistry. All peptides were subjected to mass spectrometry for identification; masses were within 1 Da of the calculated ones. The peptides were essentially pure as judged by mass spectrometry and rechromatography on HPLC.

Turn prediction in the peptides

Peptides were analyzed for their propensity to adopt a type I or II β-turn conformation as described by Wilmot and Thornton (1988). The results are indicated in Figure 1. The predictions indicate for peptide 1, a type I or II β-turn at QPGQ and, for peptide 2, a type II β-turn at GAGY and a type I at YPTS and SPQQ. Peptide 3 is constructed from peptides 1 and 2 and turns are predicted at corresponding positions; QQGY in peptide 3 replaces the GAGY sequence in peptide 2 and is predicted to adopt a type II turn

Peptide 1:

cyclo-$P_1\ G_2\ Q_3\ G_4\ Q_5\ Q_6\ P_7\ G_8\ \mathbf{Q_9}\ G_{10}\ Q_{11}\ Q_{12}$

I or II — I or II

2 or $12*10^{-6}$ — 2 or $12*10^{-6}$

Peptide 2:

cyclo-$G_1\ Y_2\ Y_3\ P_4\ T_5\ S_6\ P_7\ Q_8\ \mathbf{Q_9}\ G_{10}\ A_{11}$

II — I — I

$1*10^{-6}$ $2*10^{-6}$ $5*10^{-6}$

Peptide 3:

cyclo-$P_1\ G_2\ \mathbf{Q_3}\ G_4\ Q_5\ Q_6\ G_7\ Y_8\ Y_9\ P_{10}\ T_{11}\ S_{12}\ P_{13}\ Q_{14}\ Q_{15}$

I or II — II — I — I

2 or $12*10^{-6}$ $3*10^{-6}$ $2*10^{-6}$ $5*10^{-6}$

Fig. 1. Amino acid sequence of the cyclic peptides that were used; the residues involved in possible β-turns are underlined. Symbols I and II indicate type I and type II β-turns, with the numbers indicating the probability of occurrence calculated according to Wilmot and Thornton (1988); only values above the thresholds defined by these authors are given. The glutamines that were starting points in the synthesis are given in bold.

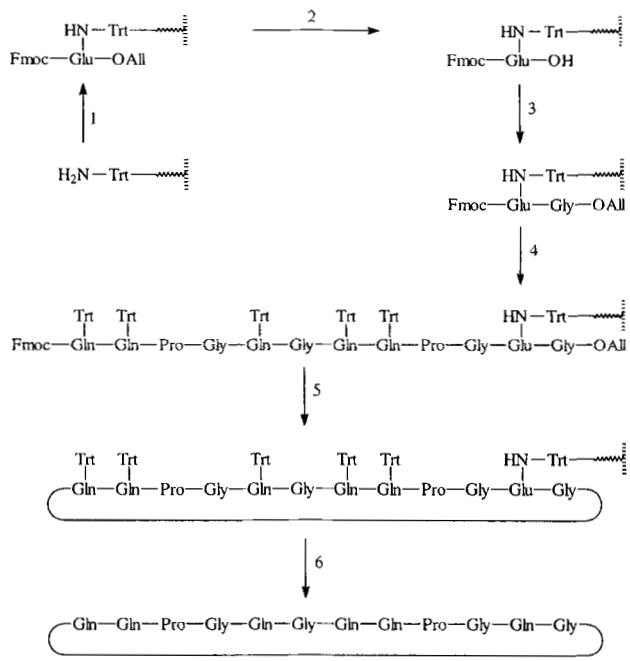

Fig. 2. Synthesis scheme for the preparation of cyclo-[PGQGQQPGQGQQ]. Other cyclic peptides were prepared using the same procedure. Experimental details are given in the text.

structure (Fig. 1). The linear peptides $(PGQGQQ)_n$ (n = 1, 3, 5) are predicted to contain the same turn structure as peptide 1.

Conformation of cyclo-PGQGQQPGQGQQ (peptide 1)

Figure 3A gives the CD spectra of peptide 1 at various concentrations. At 0.1 mg/mL, there is a minimum at 230 nm, corresponding to a $n \rightarrow \pi^*$ transition, and a maximum at 215 plus a minimum at 196 nm, corresponding to $\pi \rightarrow \pi^*$ transitions (Woody, 1996). There is a second maximum below 190 nm that might be a $\sigma \rightarrow \pi^*$ transition (Woody, 1996). The spectrum resembles a class B spectrum (Woody, 1974), indicative of a type II β-turn, but the extrema are 5 nm red shifted and the intensity of the 215 nm maximum is lower than predicted (Woody, 1974). The CD spectra show a red shift and amplitude decrease of the 196 nm minimum at high peptide concentrations (Fig. 3A), probably indicating association. The shift of only the 196-nm $\pi \rightarrow \pi^*$ transition and not the other $\pi \rightarrow \pi^*$ transition at 215 nm nor the $n \rightarrow \pi^*$ transition at 230 nm indicates that the aggregation is specific and modulates the dipole strength of only one transition; the peptide backbone conformation is most probably not affected by the aggregation. The CD spectra are independent of pH (not shown), but dependent on temperature (Fig. 3B); the 230-nm minimum and 215-nm maximum are blue shifted and the intensity of the 215-nm maximum and 196-nm minimum are both decreased at elevated temperatures. The isodichroic point at 204 nm indicates a two-state transition. The changes are compatible with proline *cis/trans* isomerization, the population of the energetically less favorable *cis*-conformation increasing with temperature.

The FTIR spectrum of peptide 1 is given in Figure 4A and its second derivative spectrum in Figure 4B; the band at 1,638 cm^{-1} is consistent with a C=O involved in a 1 ← 4 hydrogen bond in a β-turn (Hollósi et al., 1994) and supports the assignment of a

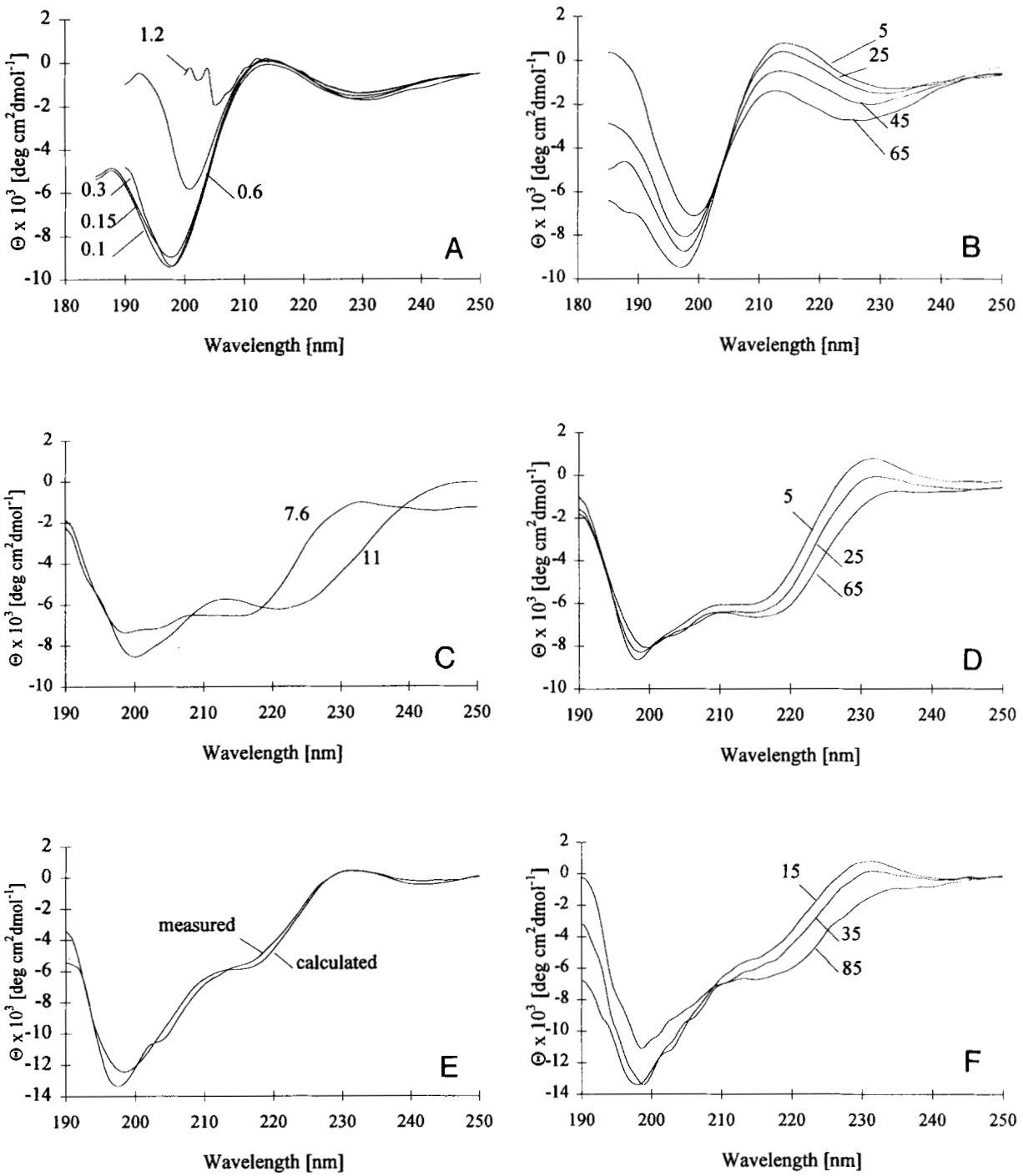

Fig. 3. CD spectra of cyclic peptides; samples contained 0.1 mg/mL peptide in 20 mM NaP_i, pH 6.0, unless indicated otherwise. Panels represent spectra of cyclo-[PGQGQQPGQGQQ] as function of concentration at 25 °C, pH 6.0 (**A**) and temperature, pH 6.0 (**B**); cyclo-[GYYPTSPQQGA] at 25 °C as function of pH (**C**) and temperature, pH 6.0 (**D**); cyclo-[PGQGQQGYYPTSPQQ] experimental versus calculated (**E**) and as function of temperature, pH 6.0 (**F**).

type II β-turn from the CD spectra. Glutamine side-chain amides absorb in the amide I region (Chirgadze et al., 1975) and may contribute significantly to the amide I band intensity of peptide 1; the shoulder at 1,620 cm^{-1} in the second derivative spectrum (Fig. 4B) may reflect such side-chain contributions. The shoulder is also observed in the spectra of the homologous peptides 4–6, which will be discussed later. The small peak at 1,659 cm^{-1} is at too high wave numbers to originate from glutamine side-chain

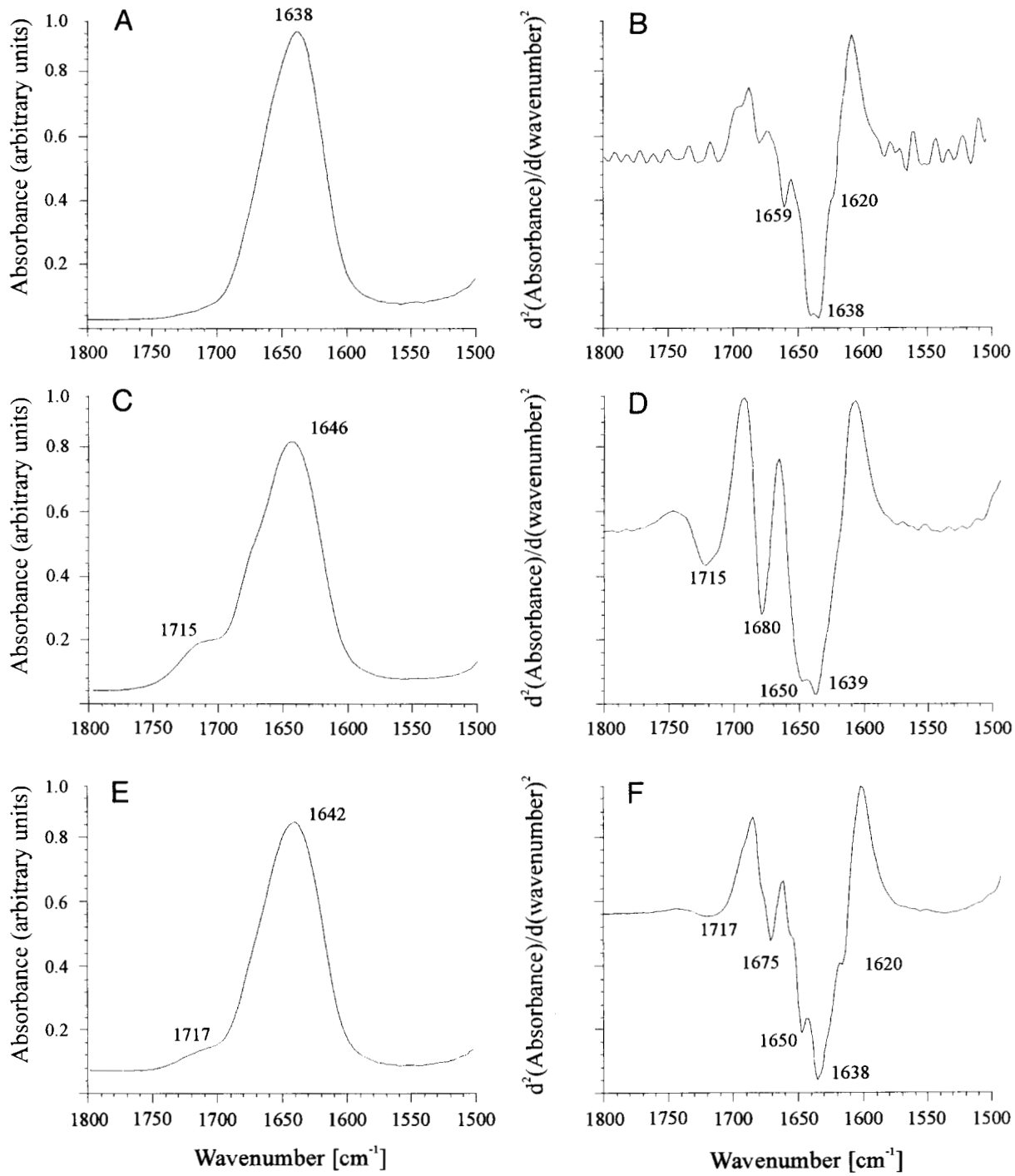

Fig. 4. Fourier transform infrared spectra in D_2O, pH 4.5, at room temperature of cyclo-[PGQGQQPGQGQQ] (2 mg/mL, **A,B**), $(PGQGQQ)_1$ (6 mg/mL, **C,D**), and $(PGQGQQ)_6$ (5 mg/mL, **E,F**). Panels represent absorption (A,C,E) and second derivative spectra (B,D,F).

amides and may reflect minor contributions from structures arising from, e.g., proline *trans/cis* isomerization.

The NH-CH^{α} region of the NMR TOCSY spectrum of peptide 1 is given in Figure 5A. Its 1D NMR spectrum is independent of peptide concentration between 0.4 and 2.0 mg/mL, indicating that the peptide conformation is independent of the concentration; this supports the interpretation of the concentration dependence of the CD spectra. A maximum of 10 cross peaks is expected in this region (the two prolines have no amide proton), but only 5 are observed, suggesting that the PGQGQQ blocks in peptide 1 are equivalent. Assignments are given in Tables 1 and 2 and connectivities in Figure 6A. The assignment of connectivities is ambiguous because residues at positions i and $(i + 6)$ are equivalent. Most connectivities could be interpreted as sequential and, because

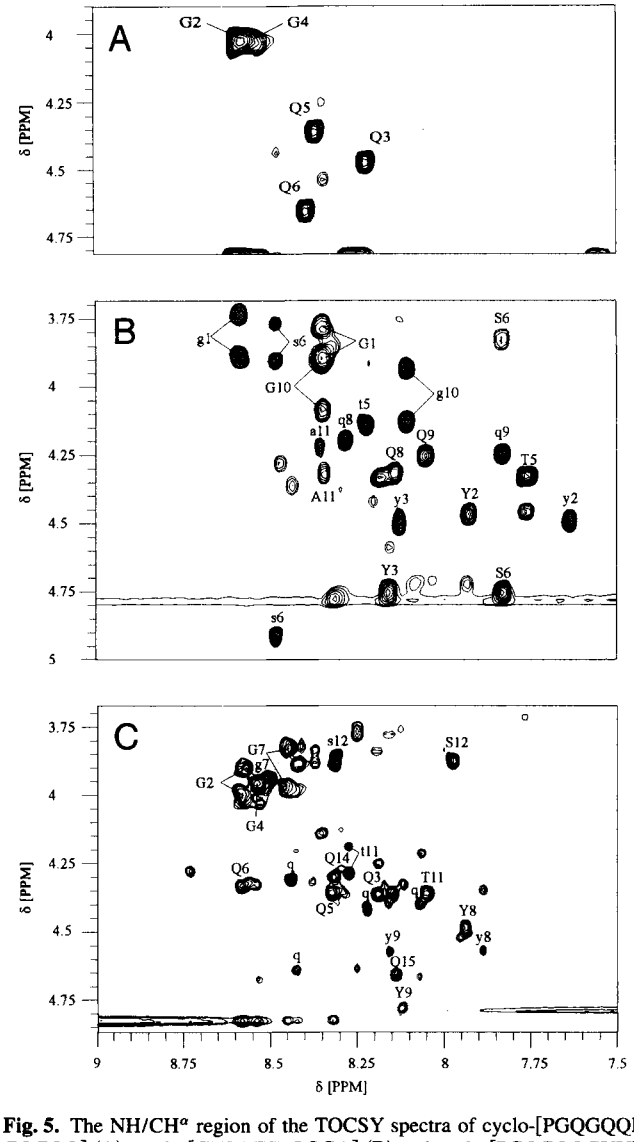

Fig. 5. The NH/CH$^{\alpha}$ region of the TOCSY spectra of cyclo-[PGQGQQP GQGQQ] (**A**), cyclo-[GYYPTSPQQGA] (**B**) and cyclo-[PGQGQQGYYP TSPQQ] (**C**). Samples contained 2.0–5.0 mg/mL peptide in 20 mM NaP_i, pH 6.5. Spectra were recorded at 20 °C as described in the Materials and methods. YPTS-proline occurs in *trans* and *cis* conformation; capital letters indicate the residues in *trans*-conformation, lower-case letters those in the *cis*-conformation.

these are the most likely to occur, they were interpreted as such. Long-range connectivities were observed from Q5 CHα to P7 CH$^{\alpha}$ and G8 NH with ambiguities as explained above. The prolines are in the *trans* conformation; this is evidenced by their CH$^{\alpha}$ resonance position at 4.40 ppm (Table 1) and the $^{13}C^{\gamma}$ at 26.3 ppm (not shown), which are typical values found for *trans* prolines (Howarth & Lilley, 1978; Dyson et al., 1988). The temperature dependence of amide resonances provides information about their involvement in hydrogen bond formation (Ohnishi & Urry, 1969); a free amide will have a temperature coefficient of −9 ppb/K, whereas values of −4 ppb/K or higher indicate hydrogen bond involvement. The coefficients of peptide 1 are given in Table 1 and Figure 7A; the one for Q3 (−1.36 ppb/K) indicates hydrogen bonding and is compatible with a type II β-turn structure with Q3 at the $(i + 3)$ position. The type II β turn structure should also give rise to specific connectivities (Dyson et al., 1988 and references sited therein), such as d_{NN} for G2/Q3, $d_{\alpha N}$ for P1/Q3 and P1/G2, all of which are observed. The connectivities are, however, ambiguous and cannot be used to identify the turn positively. The $^3J_{N\alpha}$ coupling constants could provide additional information for the turn location, but all couplings were between 4.5–7.0 Hz, which are not helpful for turn assignment; this is not uncommon for peptides (Dyson et al., 1988).

Conformation of cyclo-GYYPTSPQQGA (peptide 2)

The CD spectrum of peptide 2 is shown in Figure 3C at 25 °C and at two pH values. The 190–250-nm region contains contributions from the tyrosine rings and the peptide backbone. Apart from a broad band at ~280 nm, tyrosines normally show two absorption minima representing $\pi \rightarrow \pi^*$ transitions, one around 230 nm and one close to 190 nm (Woody & Dunker, 1996). The two equivalent tyrosines in peptide 2 are close enough for electronic interactions; instead of one absorption band, these interactions give rise to a couplet, two coupled absorption bands with equal intensity but opposite sign (Woody & Dunker, 1996). One of the couplet bands is observed at pH 7.6 at 232 nm (Fig. 3C); its negative counterpart is in the 210–230-nm region, but the negative band around 215 nm is too intense to originate from this couplet band alone. It must contain additional contributions from the peptide backbone. The minimum at 198 nm reflects a tyrosine $\pi \rightarrow \pi^*$ transition. The peptide backbone has negative ellipticity in the region 200–230 nm, which is compatible with a type C spectrum (Woody, 1974) and is associated with a type I β-turn. A type C spectrum has a positive $\pi \rightarrow \pi^*$ band around 190 nm, a part of which is observed in Figure 3C. The spectrum changes between pH 9 and 10; the spectrum at pH 11 is shown in Figure 3C. The changes are caused by deprotonation of the tyrosine rings, which was confirmed by fluorescence and UV absorbance measurements. The couplet bands have disappeared and a weak tyrosinate band is now observed at 235 nm; the tyrosine $\pi \rightarrow \pi^*$ transition in the 190–200-nm region is still observed. Figure 3D shows the temperature dependence at pH 6 of the CD spectrum; changes probably reflect primarily a reduced contribution of the tyrosine rings due to an increased mobility. This explanation is supported by a strong reduction of the tyrosine CD band at 278 nm (not shown).

The FTIR spectrum of peptide 2 shows an amide I band at 1,642 cm^{-1} (Table 3) that is compatible with a C=O involved in 1 ← 4 hydrogen bond (Hollósi et al., 1994) and supports the assignment of a type I β-turn from the CD spectra. The amide I band is broader for peptide 2 (58 cm^{-1} at half peak height) than for peptide 1 (50 cm^{-1}), indicating greater conformational heterogeneity. Second derivative analysis showed no indication of glutamine side-chain contributions to the amide I band, indicating that these are either insignificant, or that they occur at the amide I band position.

The NH-CH$^{\alpha}$ region of the NMR TOCSY spectrum is shown in Figure 5B. The 11 residues of peptide 2 can give rise to 9 cross peaks (the two prolines have no amide proton), but 18 intense cross peaks are observed, indicating that the peptide is present in two conformations, which explains the relatively broad amide I band. Assignments are summarized in Tables 1 and 2; connectivities are given in Figure 6B. Two sets of cross peaks were identified, shown in grey and white in Figure 5B, corresponding to two conformations. The P4 CH$^{\alpha}$ resonances are at 4.40 and 3.94 ppm, which are typical values for proline *trans* and *cis* isomers, respectively (Dyson

Table 1. *^{1}H chemical shifts (δ, ppm) and amide temperature coefficients (Δδ/ΔT, ppb/K) for cyclo-[PGQGQQPGQGQQ], cyclo-[GYYPTSPQQGA], and cyclo-[PGQGQQGYYPTSPQQ] at 20 °C*[a]

		cyclo(PGQGQQ)$_2$						cyclo(PGQGQQGYYPTSPQQ)					
			trans			*cis*			*trans*			*cis*	
Residues		Δδ/ΔT	δ		Δδ/ΔT	δ		Δδ/ΔT	δ			δ	
Pro	CH^{α}		4.41						4.43				
	CH^{β}		2.30	1.95					2.29	1.95			
	CH^{γ}		2.09	2.01					2.07				
	CH^{δ}		3.82	3.69					3.77	3.67			
Gly	NH	−4.97	8.63					−4.95	8.58				
	CH^{α}		4.05	3.91					4.02	3.91			
Gln	NH	−1.36	8.21					−1.54	8.15				
	CH^{α}		4.44						4.36				
	CH^{β}		2.19	1.99					2.13	1.98			
	CH^{γ}		2.33						2.33				
	NH^{δ}	−3.09	7.56	6.88					7.50	6.84			
Gly	NH	−4.97	8.62					−4.39	8.54				
	CH^{α}		3.97	3.92					3.96				
Gln	NH	−3.62	8.36					−3.82	8.33				
	CH^{α}		4.34						4.36				
	CH^{β}		2.16	1.98					2.11	1.98			
	CH^{γ}		2.32						2.34				
	NH^{δ}	−3.09	7.55	6.88					7.50	6.84			
Gln	NH	−4.79	8.42					−5.00	8.59				
	CH^{α}		4.67						4.33				
	CH^{β}		2.40	2.17					2.12	2.01			
	CH^{γ}		1.91						2.39				
	NH^{δ}	−2.98	7.56	6.90					7.57	6.89			
			cyclo(GYYPTSPQQGA)										
Gly	NH	−5.67	8.38		−5.76	8.62		−4.56	8.45		8.32		
	CH^{α}		3.95	3.83		3.94	3.79		3.98	3.83	3.89		
Tyr	NH	−2.51	7.96		0.77	7.69		−1.59	7.94		7.88		
	CH^{α}		4.51			4.55			4.49		4.57		
	CH^{β}		2.89			3.09	2.18		2.86		3.02	2.86	
	CH^{δ}		7.02			7.08			7.00		na		
	CH^{ϵ}		6.82			6.83			6.80		na		
Tyr	NH	−4.29	8.18		−4.59	8.16		−3.86	8.12		8.15		
	CH^{α}		4.78			4.56			4.78		4.58		
	CH^{β}		3.13	2.90		2.96			3.06	2.81	2.95	2.91	
	CH^{δ}		7.17			7.17			7.13		na		
	CH^{ϵ}		6.87			6.84			6.82		na		
Pro	CH^{α}		4.40			3.94			4.42		3.98		
	CH^{β}		2.37	2.00		1.98	1.84		2.31	1.96	1.97	1.79	
	CH^{γ}		2.05	2.02		1.81	1.77		2.03		1.81	1.78	
	CH^{δ}		3.63	3.52		3.56	3.44		3.57	3.48	3.54	3.40	
Thr	NH	−2.49	7.79		−5.31	8.24		−3.79	8.05		8.28		
	CH^{α}		4.39			4.19			4.37		4.29		
	CH^{β}		4.49			4.19			4.37		4.19		
	CH^{γ}		1.25			1.28			1.24		1.23		
Ser	NH	−0.38	7.87		−4.82	8.51		0.59	7.98		8.53		
	CH^{α}		4.78			4.92			4.83		4.80		
	CH^{β}		3.88			3.95	3.83		3.88		3.88		
Pro	CH^{α}		4.45			na			4.43				
	CH^{β}		2.36	2.02		na			2.32	1.94			
	CH^{γ}		2.07			na			2.03				
	CH^{δ}		3.80			na			3.84	3.74			
Gln	NH	−0.87	8.10		−2.80	8.32		−3.79	8.32				
	CH^{α}		4.31			4.25			4.30				
	CH^{β}		2.00	1.85		2.12	2.00		2.11	1.97			
	CH^{γ}		2.28			2.38			2.35				
	NH^{δ}	−2.91	7.51	6.88	−4.01	7.57	6.92		7.55	6.87			
Gln	NH	−2.11	8.18		1.06	7.88		−3.83	8.13				
	CH^{α}		4.36			4.29			4.66				
	CH^{β}		2.12	2.01		1.91	1.86		2.13	1.93			
	CH^{γ}		2.35			2.12			2.38				
	NH^{δ}	−2.66	7.50	6.85	−1.52	7.22	6.70		7.53	6.89			
Gly	NH	−4.22	8.37		−2.87	8.15							
	CH^{α}		4.13	3.95		4.18	3.98						
Ala	NH	−5.85	8.37		−5.85	8.38							
	CH^{α}		4.37			4.28							
	CH^{β}		1.41			1.43							

[a]The *cis*-conformation of cyclo-[PGQGQQPGQGQQ] was not assigned and the *cis*-conformation of cyclo-[PGQGQQGYYPTSPQQ] could only partly be assigned because of spectral overlap and too low signal intensities. The amide temperature coefficients were determined by recording spectra at different temperatures between 5 and 40 °C. n.a., not assigned.

Table 2. *^{13}C and ^{15}N chemical shifts (δ, ppm) for cyclo-[PGQGQQPGQGQQ], cyclo-[GYYPTSPQQGA], and cyclo-[PGQGQQGYYPTSPQQ] for as far as they could be determined*[a]

Residue	*trans* δ ^{15}N	δ $^{13}C^{\alpha}$	*cis* δ ^{15}N	δ $^{13}C^{\alpha}$	*trans* δ ^{15}N	δ $^{13}C^{\alpha}$
	cyclo(PGQGQQ)$_2$				cyclo(PGQGQQGYYPTSPQQ)	
Pro		62.1				62.0
Gly	nd	43.5			105.4	43.7
Gln	nd	54.1			115.3	54.1
Gly	nd	44.1			105.6	43.7
Gln	nd	54.4			115.9	54.5
Gln	nd	52.3			117.7	54.1
	cyclo(GYYPTSPQQGA)					
Gly	105.8	43.5	103.5	43.7	106.0	43.4
Tyr	115.6	56.4	115.2	56.2	116.0	56.2
Tyr	118.1	na	119.4	54.6	119.1	na
Pro		63.1		61.5		62.0
Thr	103.8	60.3	113.0	62.1	106.6	60.2
Ser	113.5	na	114.1	54.0	114.1	na
Pro		62.6		na		61.8
Gln	113.8	54.5	111.9	55.5	114.7	54.5
Gln	116.1	54.4	114.5	54.5	117.5	51.8
Gly	105.8	43.7	104.2	43.3		
Ala	118.8	51.1	118.8	51.7		

[a]n.a., not assigned; n.d., not determined.

et al., 1988); the P7 CH^{α} resonance is at 4.45 ppm in one conformation, but could not be assigned in the other due to spectral overlap. The $^{13}C^{\gamma}$ resonances of P4 are at 25.7 to 23.0 ppm (not given in Table 3), again indicating *trans/cis* isomerization (Howarth & Lilley, 1978); the $^{13}C^{\gamma}$ resonance of P7 is at 25.9 ppm in both conformations (not given in Table 3). The two conformations therefore originate from P4 *cis/trans* isomerization and will be referred to as the *cis* and *trans* conformation. They are almost equally

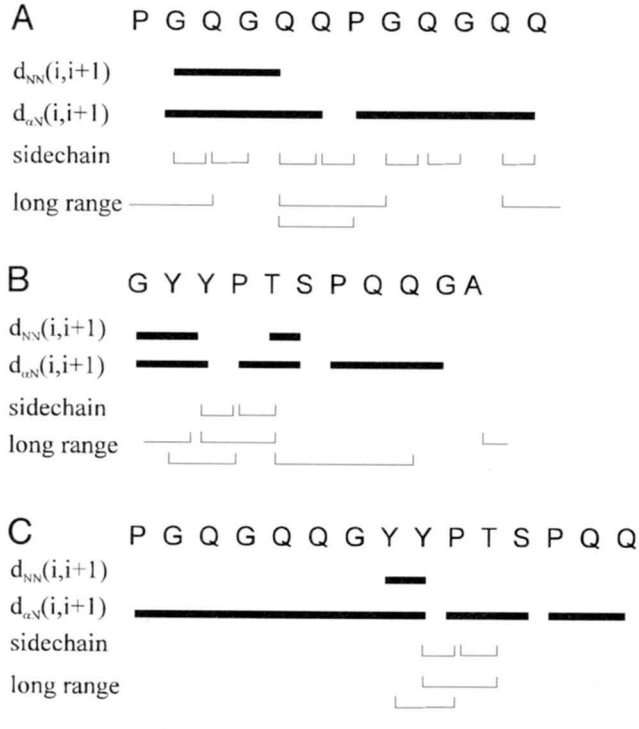

Fig. 6. Observed ^{1}H-connectivities for cyclo-[PGQGQQPGQGQQ] (**A**), cyclo-[GYYPTSPQQGA] (**B**), and cyclo-[PGQGQQGYYPTSPQQ] (**C**). Only the connectivities for the proline *trans*-conformations of the peptides are given.

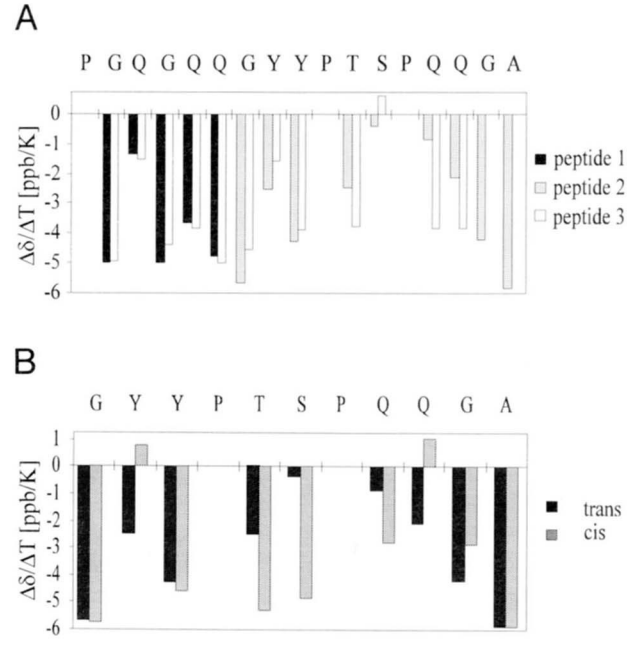

Fig. 7. NMR amide temperature coefficients for cyclo-[PGQGQQPGQGQQ], cyclo-[GYYPTSPQQGA], and cyclo-[PGQGQQGYYPTSPQQ] (**A:** only the values for the proline *trans*-conformations are given); cyclo-[GYYPTSPQQGA] in *trans*- and *cis*-conformation of the first proline (**B**).

Table 3. *Peptide amide I band positions, as determined from the corresponding FTIR spectra using second derivative analysis*[a]

Peptide number	Composition	Amide I band (cm^{-1})
1	cyclo(PGQGQQ)$_2$	1,638
2	cyclo(GYYPTSPQQGA)	1,642
3	cyclo(PGQGQQGYYPTSPQQ)	1,641
4	(PGQGQQ)$_1$	1,646
5	(PGQGQQ)$_3$	1,644
6	(PGQGQQ)$_5$	1,642

[a]Peptides were dissolved in D_2O (3–5 mg/mL) at pH 4.5; spectra were recorded at room temperature.

populated, as evidenced by comparable peak intensities in the TOCSY spectra; an unusually high *cis*-population is often observed for prolines C-terminal to tyrosines (Dyson et al., 1988). Connectivities for the *trans* conformation (Fig. 6B) are mainly sequential and are not sufficient to allow a detailed structure determination. This is even more the case for the *cis*-conformation (not shown). The NMR spectrum showed additional resonances (Fig. 5B) that were too weak to be assigned; they most probably originate from *cis/trans* isomerization at P7. The most intense of these signals could be identified as glutamines, but no site-specific assignments could be made.

The amide temperature coefficients were determined for both the *cis* and *trans* conformation (Table 1; Fig. 7B). In the *trans* conformation, the coefficient for S6 (−0.39 ppb/K) is strongly indicative for hydrogen bonding and would be compatible with its position at the (i + 3) position in a β-turn. The temperature coefficients for Y2 (−2.51 ppb/K) and Q9 (−2.11 ppb/K) also indicate hydrogen bonding and are compatible with their involvement at the (i + 3) position of a β-turn. The *trans* conformer contains three possible turns: GAGY, YPTS, and SPQQ; their presence is supported by the presence of characteristic d_{NN} connectivities between T5/S6 and G1/Y2 and $d_{\alpha N}$ connectivities between P4/S6 and P7/Q9. Some characteristic turn connectivities could not be assigned due to spectral overlap; e.g., the CH$^{\alpha}$ of Q9 (*trans*) and A11 (*trans*) overlap at 4.37/4.38 ppm (Table 1) as well as the amides of G1 (*trans*) and A11 (*cis*) at 8.38 ppm making the assignment of the expected A11/G2 $d_{\alpha N}$ connectivity ambiguous. The coefficients for T5 and Q8 are also low (Fig. 7A; Table 1) but their occurrence in the (i + 3) position of a type I or II β-turn is unlikely because it would require a proline at the (i + 2) position (Wilmot & Thornton, 1988). A possible explanation for the low coefficient for the T5 NH might be that ring current interactions with one of the tyrosine rings occur; when the relative orientation of the amide and the aromatic ring changes with temperature this will affect the apparent temperature coefficient. A similar phenomenon has been reported for the C4H imidazole proton of His 76 in the *Escherichia coli* protein HPr (Dooijewaard et al., 1979). The T5 NH has an abnormal ^{15}N resonance position at 103.8 ppm (Table 2) that shifts to 112.9 ppm in the *cis* conformation (Table 2), compatible with a structural change. Its amide temperature coefficient changes from −2.49 to −5.31 ppb/K (Table 1), which would be compatible with a changing interaction between the T5 NH and the tyrosine ring. The origin of the low temperature coefficient for Q8 remains unclear.

When the conformation changes from *trans* to *cis*, the turn structure at YPTS is lost and is reformed at SPQQ. This is evidenced by the temperature coefficient of S6, which changes from −0.38 to −4.82 ppb/K, the largest change observed (Fig. 7B) indicating the loss of hydrogen bonding. At the same time, the coefficients for Y2 and Q9 change from −2.52 to +0.77 ppb/K (Y2) and −2.11 to +1.06 ppb/K (Q9), indicative of increasing hydrogen bonding strength. The temperature coefficient of the side-chain amide of Q9, the (i + 3) residue in the SPQQ turn, is reduced significantly from −2.66 to −1.55 ppb/K, which is compatible with hydrogen bond formation between this group and the S6 backbone C=O, as is often observed for glutamines at this position in β-turns (Wilmot & Thornton, 1988). Summarizing, the *trans/cis* isomerization results in a loss of the turn structure at YPTS with increasing turn character at GAGY and SPQQ.

Conformation of cyclo-PGQGQQGYYPTSPQQ (peptide 3)

Peptide 3 is the fusion of peptide 1 and 2 with a PGQGQQ unit from peptide 1 and the GYYPTSPQQ unit from peptide 2 (Fig. 1). The CD spectrum of peptide 3 is shown in Figure 3E, together with the calculated spectrum using the normalized data for peptides 1 and 2. The experimental and calculated spectra are similar, indicating that the turn structures of the two building blocks (peptides 1 and 2) are preserved. The CD spectrum is not concentration dependent; the pH dependence is similar to that of peptide 2, reflecting tyrosine deprotonation. The temperature dependence is given in Figure 3F and shows the combined effects for peptides 1 and 2. The FTIR spectrum of peptide 3 shows an amide I band at 1,641 cm^{-1} (Table 3), intermediate between the position for peptide 1 (1,638 cm^{-1}) and peptide 2 (1,642 cm^{-1}) and compatible with β-turn structure (Hollósi et al., 1994). The band width is 54 cm^{-1} intermediate between the 50 cm^{-1} for peptide 1 and the 58 cm^{-1} for peptide 2. Second derivative analysis did not show a separate contribution of glutamine side-chain amides, indicating that it is either insignificant or occurs at the amide I band position.

The NH-CH$^{\alpha}$ region of the NMR TOCSY spectrum is shown in Figure 5C. Two conformations were identified originating from *cis/trans* isomerization at P10, as derived from the characteristic shifts in resonance position of its CH$^{\alpha}$ at 4.42 and 3.98 ppm (Table 1) and analogous to the equivalent P4 in peptide 2. Cross peak intensities indicate that 80% of the population is in the *trans* conformer, which could be completely assigned (Table 1; Fig. 6C); the *cis* conformer could only be assigned partly due to overlap and the relatively low signal intensities. The resonance position of the CHα protons in peptide 3 and those of the corresponding residues in peptide 1 and 2 are similar (Table 1), supporting the preservation of the structure of peptides 1 and 2 in peptide 3. The amide temperature coefficients were determined (Table 1; Fig. 7A), showing low values for Q3, Y8, and S12, as expected from the results for peptide 1 and 2. The coefficient for S12 is higher in peptide 3 than for its equivalent in peptide 2 (+0.59 versus −0.38 ppb/K), indicating a stronger hydrogen bond in peptide 3; this is compatible with the observed higher population of the *trans* conformer. The temperature coefficient for Q15 in peptide 3 (Fig. 1) is higher than that of the corresponding residue in peptide 2, indicating reduced hydrogen bonding at SPQQ in peptide 3 relative to peptide 2. Connectivities that are characteristic for type I and II β-turn structures could only be identified partly due to spectral overlap, similar to the situation for peptides 1 and 2.

Conformational analysis of $(PGQGQQ)_n$ (n = 1, 3, 5) (peptides 4, 5, 6)

Linear forms of peptide 1 were produced; their CD spectra are given in Figure 8A. The spectrum of $(PGQGQQ)_1$ shows a maximum at 210 nm and a minimum at 193 nm, with intensities much like that of random coil structure (Woody, 1996). When the number of PGQGQQ-units increases to 3 or 5, the 193-nm and 210-nm extrema are red shifted to 196 nm and 213 nm, respectively, and reduced in amplitude; in addition, a weak minimum develops at 230 nm. The spectrum of peptide 6 is similar to that of peptide 1 (Fig. 3A), indicating their structural similarity. The amide I band of peptides 4–6 (Table 3) shifts from 1,646 cm^{-1} (peptide 4) to 1,644 $^{cm-1}$ (peptide 5) and 1,642 cm^{-1} (peptide 6), compatible with increasing hydrogen bonding character as in a 1 ← 4 hydrogen bond in a β-turn (Hollósi et al., 1994). Second derivative spectra of peptides 4 and 6 (Fig. 4 D,F) show that the amide I band is composed of bands 1,650 cm^{-1}, associated with random coil, and 1,638 cm^{-1} (1,639 cm^{-1} for peptide 4), the position where the amide I band of peptide 1 was observed. As for peptide 1, a shoulder is observed at 1,620 cm^{-1}, which is most prominent for peptide 6 (Fig. 4F), but is also found for peptide 4 (Fig. 4D). The intensity of the band at 1,638 cm^{-1} increases with chain length relative to that of the band at 1,650 cm^{-1} (Fig. 4D,F). The CD and FTIR data indicate a chain length-dependent conformational stabilization; the cyclic peptide 1 possibly is a stabilized form of the linear peptides 4–6. The spectra in Figure 4C and E show a band at 1715–1717 cm^{-1}, which was not observed in the FTIR spectrum of peptide 1 (Fig. 4A). Second derivative analysis shows an additional band at 1,680–1,675 cm^{-1}. Apart from length, the only differences between peptide 1 and peptide 4–6 are the C-terminal carboxylate and the N-termial NH_2 groups, which are absent in the cyclic peptide. The carboxylate probably gives rise to both bands; their intensity relative to that of the amide I band is decreasing with chain length, as expected. Two bands for one carboxylate have also been observed by Chirgadze and Brazhnikov (1973) for several peptides and they indicate local structural heterogeneity at the carboxylate. The NH-CHα region of the TOCSY spectrum of peptide 6, shown in Figure 8B, strongly resembles that of peptide 1 (Fig. 5A), indicating their structural similarity. The peaks are broad, indicating some conformational heterogeneity. Separate resonances, marked with an * in Figure 8B, are observed for the first glycine and glutamine at the N-terminus; in addition, the CH^{α}-CH^{β} region contains a separate set of resonances for the first proline. The N-terminal structure of peptide 6 seems to be different from the rest of the peptide.

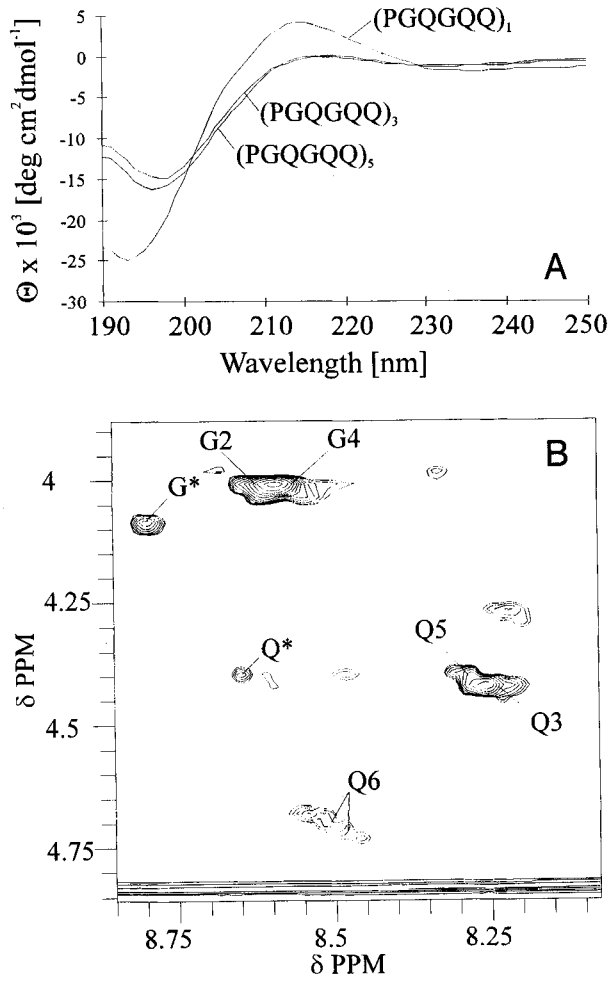

Fig. 8. Spectra of $(PGQGQQ)_{1,3,5}$. CD spectra (**A:** samples contained 0.05–0.2 mg/mL peptide in 20 mM NaPi, pH 6.0, at 25 °C); NH/CH^{α} region of the TOCSY spectrum of $(PGQGQQ)_5$ (**B:** 3.0 mg/mL in 20 mM NaP_i, pH 6.5, at 20 °C).

Discussion

Using a novel synthesis route, cyclic peptides were synthesized that represent the HMW consensus sequences. The data presented show that cyclo-[PGQGQQPGQGQQ] (peptide 1, Fig. 1) contains a type II β-turn located at the residues QPGQ. The glutamine at position (*i* + 3) most probably forms an additional stabilizing hydrogen bond to the residue at the first position through its side-chain amide (Wilmot & Thornton, 1988). The type II β-turn structure is also present in the linear peptides $(PGQGQQ)_n$ (*n* = 1, 3, 5) and is more prominent at higher *n* values, clearly demonstrated by the shifting of the amide I band (Table 3). In peptide 1, long-range contacts were observed from Q5 to P7 and G8 indicating that they are close. Even though Q5 is not involved in the β-turn that involves P7 and G8, its position is restricted, possibly by hydrogen bonding of its side-chain amide with the peptide backbone. The structure of peptide 1 seems to be restricted not only at the β-turn, but also in the region between the turns as a result of additional hydrogen bonding. These interactions may be the origin of the observed chain length-dependent structural stabilization in the linear peptide $(PGQGQQ)_n$. The structure in peptides 1, 5, and 6 thus would be unusually highly stabilized by hydrogen bonds, which might explain the reduced amplitude of the 215-nm maximum and the red shift of the CD spectrum relative to that of the calculated type B CD spectrum (Woody, 1974).

Peptides 2 and 3 (Fig. 1) show a complicated turn composition and, in addition, *cis/trans* isomerization at the proline in the YPTS sequence. When this proline is in the *trans* conformation, it is involved in a type I β-turn; there is indication for additional turns at SPQQ and GAGY (peptide 2) or QQGY (peptide 3). The CD spectrum of peptide 2 indicates type I β-turn character, which would agree with the predictions for the YPTS and SPQQ sequences (Fig. 1). The predictions for GAGA (peptide 2), however, indicate type II β-turn; its presence could be partly responsible for

the deviation of the peptide 2 CD spectrum from the calculated type I β-turn spectrum (class C according to Woody, 1974) and for its relatively broad amide I band. However, other factors also contribute to these phenomena, as explained in the Results. The turn conformation at GAGY can therefore be either type I or type II. When the configuration at YPTS changes from *trans* to *cis*, its turn structure is lost, but the turn character at SPQQ and GAGY (peptide 2) or QQGY (peptide 3) is increased. Peptides 2 and 3 may contain overlapping turns, which is a phenomenon that has also been observed in proteins (Isogai et al., 1980).

Tatham et al. (1990) performed measurements with linear HMW consensus peptides in aqueous solutions. Their FTIR spectra for the linear peptide GQQPGQG, the equivalent of peptide 1 (Fig. 1), showed a band at 1,641 cm^{-1}, which they interpreted as indicative for unordered structure (Tatham et al., 1990), but which is now known to be compatible with turn structure (Holósi et al., 1994). This agrees well with our data for the linear peptides $(PGQGQQ)_{1,3,5}$. Tatham et al. (1990) also obtained data in aqueous solutions for the peptides GQPGYYPTSP and GQQGYYPTSP, equivalents of peptide 2 (Fig. 1). Their CD spectra are comparable to those for peptide 2; their FTIR data showed amide bands around 1,640 cm^{-1}, which are now known to be compatible with β-turn structure (Holósi et al., 1994) and are in agreement with our data for the cyclic peptide 2.

Materials and methods

Materials

Fmoc-amino acids were from Bachem (Bubendorf). DIPCDI and HOBt were from Fluka. Other chemicals were obtained from Sigma and Merck and were analytical grade or better.

Thin layer chromatography (TLC)

TLC was performed using Kieselgel 60 F_{254} plates. Spots were visualized by UV quenching (indicated as UV), spraying with H_2SO_4/MeOH (1/1) and heating (indicated as H^+, detection of trityl cations), spraying with ninhydrine solution (indicated as Nin, demonstration of free NH_2) or with chlorine/TDM/KI solution (indicated as TDM, demonstration of NH).

Synthesis of $^+H_2$-Gly-OAll,TosO$^-$

The synthesis was conducted according to Waldmann and Kunz (1983); 100 mmol H-Gly-OH, 110 mmol pTOS, and 100 mL freshly distilled allyl alcohol were dissolved in 50 mL benzene. The reaction mixture was refluxed for 24 h under separation of water and subsequently evaporated in vacuo. The resulting oil crystallized in ether. Yield: 97%. Mp.: 73–74 °C. R_f(BuOH/AcOH/H_2O = 4/1/1): 0.51.

Synthesis of Fmoc-Glu-OAll

Synthesis of Trt-Glu(OAll)-OAll

$^+H_2$-Glu(OAll)-OAll,TosO$^-$ (9.97 g, 25 mmol), prepared as described by Waldmann and Kunz (1983), was dissolved in DCM (30 mL) and triethylamine (6.95 mL, 50 mmol) was added. The clear solution was cooled on ice. Trt-Cl (7.65 g, 27.5 mmol), dissolved in 20 mL DCM, was added dropwise under stirring, during which the solution became slightly warm and turbid. After stirring for 60 min, the reaction was stopped by adding 5 mL of MeOH. The salt dissolved and the reaction mixture was evaporated in vacuo. The pale yellow oil was dissolved in diethylether and water (100 mL each). The water layer was extracted with diethylether (2 × 100 mL) and the collected ether fractions were washed successively with water (2 × 200 mL), 1% citric acid (2 × 200 mL), a saturated $NaHCO_3$-solution (2 × 100 mL), and a saturated NaCl-solution (2 × 100 mL), then dried on Na_2SO_4, filtered, and evaporated in vacuo yielding a yellow oil (11.2 g, 23.9 mmol). Yield: 95%. α_D = +36.6 (c = 1.175 mg/mL, $CHCl_3$). R_f(BuOH/AcOH/H_2O = 4/1/1): 0.90 UV, Nin, TDM, H^+; R_f($CHCl_3$/MeOH = 9/1): 0.90 UV, Nin, TDM, H^+.

Synthesis of H-Glu-OAll

Trt-Glu(OAll)-OAll (4.70 g; 10 mmol) was dissolved in 25 mL glacial acetic acid; 1 mL of concentrated HCl and 3 mL of water were added and the reaction mixture was stirred for 10 min at 80 °C. Water was added until the Trt-OH precipitated; after cooling, the precipitated TrtOH was filtered off and the filtrate was evaporated. The resulting oil was dissolved in 50 mL water; the water layer was extracted four times with 50 mL diethylether. The water was evaporated and the resulting product (H-Glu-OAll) was converted directly into Fmoc-Glu-OAll.

Synthesis of Fmoc-Glu-OAll

The synthesis was performed as described by Paquet (1982). H-Glu-OAll (1.45 g, 7.75 mmol) was dissolved in a saturated $NaHCO_3$-solution and a small excess $NaHCO_3$. Fmoc-OSu (2.87 g, 8.5 mmol) was dissolved in acetonitrile (25 mL) and added. A two-phase system was formed that was stirred vigorously overnight. The white precipitate was filtered off. The filtrate was acidified with a 2-N $KHSO_4$-solution (CO_2 gas was formed, Na_2SO_4 precipitated); Na_2SO_4 was filtered off. The acidic solution was extracted with ethylacetate (2 × 25 mL) and the organic layer was washed with a 2-N $KHSO_4$-solution (8 × 20 mL). The ethylacetate was dried on Na_2SO_4 and evaporated in vacuo yielding a yellow oil, which was solidified with petroleumether. A white powder (1.9 g, 4.8 mmol) was formed. Yield: 56%. Mp: 87–91 °C. α_D: +0.85 (c = 11.7 mg/mL, $CHCl_3$); R_f(BuoH/AcOH/H_2O = 4/1/1): 0.83 UV, TDM.

Peptide synthesis (Fig. 2)

Coupling of Fmoc-Glu-OAll to the aminotrityl resin and subsequent removal of the allyl function

The peptide synthesis was performed as described in Figure 2. The preparation and use of the hydroxyl form of the trityl resin has been described (Van Vliet et al., 1992, 1994) and was converted to the amino form as follows. The resin was washed twice with 5% thionyl-chloride in DCM. Then 20% $SOCl_2$ in DCM was added and the resin was rotated for 2 h, followed by a 5-min wash with a fresh portion of $SOCl_2$/DCM; the resin colored orange. Then the resin was washed rapidly with 5% thionyl chloride in DCM; NH_3/DCM was added until pH > 6 and the resin colored pale yellow. After rotation for 2 h, the resin was filtered off and washed sequentially with DCM, (isopropanol, DCM, DMF, DCM)$_3$ and finally with diethylether. In the following, this procedure will be called "washed as usual." In addition, water was used to dissolve the ammonium chloride. The resin contained up to 0.5 mmol amino moieties per gram. The resin (2.0 g) was suspended in 15 mL tetrahydrofuran, and 2.0 g (5 mmol) Fmoc-Glu-OAll, and 1.1 g DCC (5.3 mmol) were added. After one night of rotation at room

temperature, the resin was washed as usual. After drying to constant weight, the Fmoc-substitution level was determined by UV analysis as described by Meienhofer et al. (1979). The remaining free trityl amino functions on the resin were capped using acetic anhydride and DIPEA until the Kaiser-test (Kaiser et al., 1970) was negative. The allyl function was removed using the procedure of Albericio et al. (1992). The resin was suspended in 21.5 mL $CHCl_3$/AcOH/NMM (20/1/0.5). Oxygen was removed by bubbling argon through the solution, after which 200 mg $Pd(PPh_3)_4$ were added. After one night of rotation at room temperature, the resin was washed as usual.

Coupling of H-Gly-OAll

Four-hundred thirty milligrams $^+H_2$Gly-OAll,TosO^- were dissolved in DCM and 265.5 μL DIPEA were added. The resin adduct was suspended in 15 mL dry DCM and 481.2 mg TBTU (1.5 mmol), 213.7 mg HOBt (1.5 mmol), the solution containing the free ester H-Gly-OAll, and 249.5 μL NMM (2.5 mmol) were added. After rotating for one night at room temperature, the resin was filtered off and washed as usual. Incorporation of H-Gly-OAll was verified by TLC, after detachment from the resin, and amino acid analysis.

Chain elongation using solid-phase peptide synthesis

The peptide was built up stepwise following the Fmoc-protocol using DIPCDI/HOBt as a coupling reagent; coupling time was 60 min. Fmoc deprotection was performed by treatment with 20% piperidine/DMF (3 × 6 min). The coupling and deprotection steps were checked by Kaiser tests (Kaiser et al., 1970). After completion of the synthesis, the allyl ester was removed as described before, using 300 mg $Pd(PPh_3)_4$, and then the N terminus was set free by treatment with 20% piperidine/DMF.

Cyclization of the peptide

The resin was suspended in 20 mL DCM and 240.6 mg TBTU (0.75 mmol), 115.9 mg HOBt (0.75 mmol), and 124.8 μL NMM (1.13 mmol) were added. After rotating for three nights at room temperature, the resin was filtered off and washed as usual.

Cleavage from the resin and removal of protecting groups

The resin was suspended in TFA/DCM/MeOH (90/6/4). After rotating for 30 min, the resin was filtered off and washed with DCM and MeOH. The filtrate was evaporated and the residue was solidified with diethylether.

Peptide purification

About 100 mg of the crude product was dissolved in 1 mL 0.1% TFA and loaded on a reversed-phase HPLC C18 column (5 × 300 mm) and eluted using a gradient of 0–60% B in A (A, 0.1% TFA in water; B, 0.1% TFA in acetonitril) with a flow of 3 mL/min. The effluent was monitored using UV-detection at 214 nm; peaks were collected and subjected to electrospray mass spectrometry for product identification.

Electro spray mass spectrometry (ES-MS)

ES-MS was performed using a home built single quadrupole mass spectrometer. Samples were sprayed as obtained after HPLC analysis.

CD measurements

CD spectra were recorded on an AVIV CD spectrometer model 62A DS equipped with an Apple Power Macintosh 7100/66 computer. The instrument was calibrated with benzene vapor (wavelength) and d-camphorsulfonic acid (magnitude). Spectra are the average of five scans recorded using a band width of 1 nm, a step width of 1 nm, and a 1-s averaging time per point. Temperature and solution conditions are specified in the figure legends.

Spectra were smoothed using a binomial smoothing algorithm as described by Marchand and Marmet (1983), repeated five times. Ellipticities showed standard deviations of 0.1 mdegrees at 250 nm to 0.3 mdegrees at 190 nm.

FTIR spectroscopy

FTIR measurements were performed essentially as described by Haris et al. (1992) using a Nicolet 174 FTIR spectrometer. Peptides were dissolved in D_2O at concentrations between 2 and 10 mg/mL. The pH of the samples was 4.0–4.5; pH measurements were not corrected for deuterium isotope effects. Data were processed using the software supplied by the manufacturer.

NMR measurements

NMR spectra were recorded on a VARIAN UNITY 500 NMR spectrometer. TOCSY spectra were recorded according to Bax and Davis (1985b) using a mixing time of 70 ms; ROESY spectra according to Bax and Davis (1985a) with mixing times of 100, 200, 300, 400, and 500 ms; natural abundance $^1H\{^{13}C\}$HSQC and $^1H\{^{15}N\}$HSQC spectra were recorded as described by Bax et al. (1990). Data were processed using software supplied by the manufacturer or using the SNARF program, developed in-house by F. van Hoesel. Samples were dissolved in 20 mM NaP_i buffer, pH 6.0, and contained 5–10 mg/mL peptide and 10% D_2O to provide an internal lock signal. Chemical shifts are relative to 2,2-dimethyl-2-silapentane-5-sulfonic acid (^1H), dioxane (^{13}C), or $(NH_4)_2SO_4$(^{15}N).

Determination of peptide concentrations

Peptide concentrations were determined using quantitative amino acid determination by Eurosequence BV, Groningen, Netherlands. Concentrations are accurate to within 10%.

Acknowledgments

This research was supported by the Dutch Ministry of Economic Affairs, project IOP-IE92014. We thank Dr. R.M. Scheek and K. Dijkstra for their assistance in the recording and interpretation of the NMR spectra.

References

Albericio F, Barany G, Fields GB, Hudson D, Kates SA, Lyttle MH, Solé NA. 1992. Allyl-based orthogonal solid phase peptide synthesis. In: Schneider CH, Eberle AN, eds. *Peptides*. Leiden, Netherlands: ESCOM Science Publishers BV. pp 191–193.

Anderson OD, Greene FC. 1989. The characterization and comparative analysis of high molecular weight glutenin genes from genomes A and B of a hexaploid bread wheat. *Theor Appl Genet 77*:689–700.

Bax A, Davis DG. 1985a. Practical aspects of two-dimensional transverse NOE spectroscopy. *J Magn Reson 63*:207–212.

Bax A, Davis DG. 1985b. MLEV-17 based two-dimensional homonuclear magnetization transfer spectroscopy. *J Magn Reson 65*:355–360.

Bax A, Ikura M, Kay LE, Torchia DA, Tschudin R. 1990. Comparison of different modes of two-dimensional reverse-correlation NMR for the study of proteins. *J Magn Reson 86*:304–318.

Chirgadze YN, Brazhnikov EV. 1973. Intensity of the infrared amide I band of dipeptides in heavy water. *Biopolymers 12*:2185–2188.

Chirgadze YN, Fedorov OV, Trushina NP. 1975. Estimation of amino acid

residue side-chain absorption in the infrared spectra of protein solutions in heavy water. *Biopolymers 14*:679–694.

Dooijewaard G, Roossien FF, Robillard GT. 1979. *Escherichia coli* phosphoenolpyruvate dependent phosphotransferase system. NMR studies of the conformation of HPr and P-HPr and the mechanism of energy coupling. *Biochemistry 18*:2669–3001.

Dyson HJ, Rance M, Houghton RA, Lerner RA, Wright PE. 1988. Folding of immunogenic peptide fragments of proteins in water solution. I. Sequence requirements for the formation of a reverse turn. *J Mol Biol 201*:161–200.

Haris PI, Robillard GT, van Dijk AA, Chapman D. 1992. Potential of ^{13}C and ^{15}N labelling for studying protein–protein interactions using fourier transform infrared spectroscopy. *Biochemistry 31*:6279–6284.

Hollósi M, Majer Zs, Rónai AZ, Magyar A, Medzihradszky K, Holly S, Perczel A, Fasman GD. 1994. CD and fourier transform IR spectroscopic studies of peptides. II. Detection of β-turns in linear peptides. *Biopolymers 34*:177–185.

Howarth OW, Lilley DMJ. 1978. Carbon-13-NMR of peptides and proteins. *Progr NMR Spectr 12*:1–40.

Isogai Y, Németh G, Rackovsky S, Leach SJ, Scheraga HA. 1980. Characterization of multiple bends in proteins. *Biopolymers 19*:1183–1210.

Kaiser E, Colescott RL, Bossinger CD, Cook PI. 1970. Color test for detection of free terminal amino groups in the solid-phase synthesis of peptides. *Anal Biochem 34*:595–598.

Marchand P, Marmet L. 1983. Binomial smoothing filter: A way to avoid some pitfalls of least-squares polynomial smoothing. *Rev Sci Instrum 54*:1034–1041.

Meienhofer J, Waki M, Heimer EP, Lambros TJ, Makofske RC, Chang CD. 1979. Solid phase synthesis without repetitive acidolysis. *Int J Peptide Protein Res 13*:35–42.

Miles MJ, Carr HJ, McMaster TC, I'Anson KJ, Belton PS, Morris VJ, Field JM, Shewry PR, Tatham AS. 1991. Scanning tunneling microscopy of a wheat seed storage protein reveals details of an unusual supersecondary structure. *Proc Natl Acad Sci USA 88*:68–71.

Ohnishi M, Urry DW. 1969. Temperature dependence of amide proton chemical shifts: The secondary structures of gramicidin S and valinomycin. *Biochem Biophys Res Commun 36*:194–202.

Paquet A. 1982. Introduction of 9-fluorenylmethyloxycarbonyl, trichloroethoxycarbonyl, and benzyloxycarbonyl amine protecting groups into O-unprotected hydroxyamino acids using succinimidyl carbonates. *Can J Chem 60*:976–980.

Perczel A, Hollósi M. 1996. Turns. In: Fasman GD, ed. *Circular dichroism and the conformational analysis of biomolecules*. New York: Plenum Press. pp 285–380.

Shewry PR, Miles MJ, Tatham AS. 1994. The prolamin storage proteins of wheat and related cereals. *Prog Biophys Mol Biol 61*:37–59.

Tatham AS, Drake AF, Shewry PR. 1990. Conformational studies of synthetic peptides corresponding to the repetitive regions of the high molecular weight (HMW) glutenin subunits of wheat. *J Cereal Sci 11*:189–200.

van Vliet A, Rietman BH, Karkdijk SCF, Adams PJHM, Tesser GI. 1994. Protected peptide intermediates using a trityl linker on a solid support II. In: Hodges RS, Smith JA, eds. *Peptides: Chemistry, structure and biology*. Leiden, Netherlands: ESCOM Science Publishers BV. pp 151–152.

van Vliet A, Smulders RHPH, Rietman BH, Tesser GI. 1992. Protected peptide intermediates using a trityl linker on a solid support. In: Epton R, ed. *Innovations and perspectives in solid phase synthesis and related technologies: Peptides, polypeptides and oligonucleotides*. Andover, UK: Intercept Andover. pp 475–477.

Waldmann H, Kunz H. 1983. Allylester als selektiv abspaltbare arboxyschutzgruppen in der peptid- und N-glycopeptidsynthese. *Liebigs Ann Chem*:1712–1725.

Wilmot CM, Thornton JM. 1988. Analysis and prediction of the different types of β-turn in proteins. *J Mol Biol 203*:221–232.

Woody RW. 1974. Studies of theoretical circular dichroism of polypeptides: Contributions of β turns. In: Blout ER, Bovey FA, Goodman M, Latan N, eds. *Peptides, polypeptides and proteins*. New York: John Wiley & Sons Inc.. pp 338–350.

Woody RW. 1996. Theory of circular dichroism of proteins. In: Fasman GD, ed. *Circular dichroism and the conformational analysis of biomolecules*. New York: Plenum Press. pp 25–68.

Woody RW, Dunker AK. 1996. Aromatic and cystine side-chain circular dichroism in proteins. In: Fasman GD, ed. *Circular dichroism and the conformational analysis of biomolecules*. New York: Plenum Press. pp 109–158.